Origins of ferromagnetism and antiferromagnetism in Gd_5Ge_4

Origins of ferromagnetism and antiferromagnetism in Gd$_5$Ge$_4$

Durga Paudyal[1], V K Pecharsky[1,2] and K A Gschneidner Jr[1,2]

[1] Ames Laboratory of the US DOE, Iowa State University, Ames, IA 50011-3020, USA
[2] Department of Materials Science and Engineering, Iowa State University, Ames, IA 50011-2300, USA

E-mail: vitkp@ameslab.gov

Abstract
The total and partial density of states (DOS) of two polymorphic modifications of Gd$_5$Ge$_4$ show varying hybridization between the 5d states of Gd and the 4p states of Ge resulting in differences in the magnetism of the compound that are consistent with changes in the chemical bonding. The integrated numbers of electrons in the minority and majority bands differ substantially from one allotrope to another, showing different magnetic moments. A substantial decrease of indirect exchange interactions between 4f spins of specific Gd atoms, which is reflected in the decrease of 5d DOS and the 5d band splitting at the Fermi level, supports the antiferromagnetic ground state of Gd$_5$Ge$_4$. As follows from calculations of 4f–5d exchange interaction energies, total energy analysis of different spin configurations, and band energy analysis, short range interactions are ferromagnetic but long range antiferromagnetic coupling between Gd atoms prevails in the ground state allotrope of Gd$_5$Ge$_4$. On the other hand, only ferromagnetic coupling is found in the high field Gd$_5$Ge$_4$ structure.

(Some figures in this article are in colour only in the electronic version)

1. Introduction

Magnetostriction, magnetoresistance and magnetocaloric effects are only a few of the interesting effects that may occur in complex magnetic materials in response to a varying magnetic field. For some time the condensed matter community has been involved in the design of nanostructured and multilayered materials with the goal of maximizing some, or all, of these magnetoresponsive phenomena [1]. On the other hand, certain intermetallic compounds, e.g. R$_5$T$_4$ where R = rare earth and T = Si, Ge, form nanolayers (nanoslabs) naturally. Most importantly and contrary to all known artificial nanolayered structures, the slabs may be rearranged by external triggers such as temperature, magnetic field and/or pressure, resulting in simultaneous magnetic and structural transitions, and drastically changing the electronic properties of such material.

Among numerous possible R$_5$T$_4$ systems, Gd$_5$Si$_x$Ge$_{4-x}$ alloys are the most studied materials, and they are well known for their strong magnetostriction, magnetoresistance and magnetocaloric effects. Initial studies of the crystallography and the basic magnetic properties of Gd$_5$Si$_x$Ge$_{4-x}$ compounds reported by Smith *et al* [2] and Holtzberg *et al* [3] in

1967 were followed by Pecharsky and Gschneidner in 1997, who discovered the giant magnetocaloric effect (MCE) in Gd$_5$Si$_2$Ge$_2$ [4]. This discovery not only highlighted the potential importance of Gd$_5$Si$_x$Ge$_{4-x}$ compounds in future energy technologies, but also offered a platform for the development and application of experimental and theoretical tools to understand the basic physics behind the intriguing phenomenology of these materials. Compared to conventional ferromagnets, the magnetoresponsiveness of R$_5$T$_4$ systems is enhanced due to a first order phase transition when ferromagnetic (FM) ordering is accompanied by a structural transformation [5, 6]. Thereafter, magnetostructural transformations at various temperatures became a subject of broad experimental investigations because of the interest in near room temperature magnetic refrigeration and other energy conversion technologies [7–10].

Experiments indicate that one of the end members of the Gd$_5$Si$_x$Ge$_{4-x}$ family, namely, the germanide Gd$_5$Ge$_4$ is antiferromagnetic (AFM) below $T_N \cong 128$ K (figure 1). Unlike other representatives of this family with $x > 0$, the germanide does not exhibit a first order AFM O(II) $\rightarrow$ FM O(I) phase transformation upon cooling down to $\sim$1.8 K as long as the
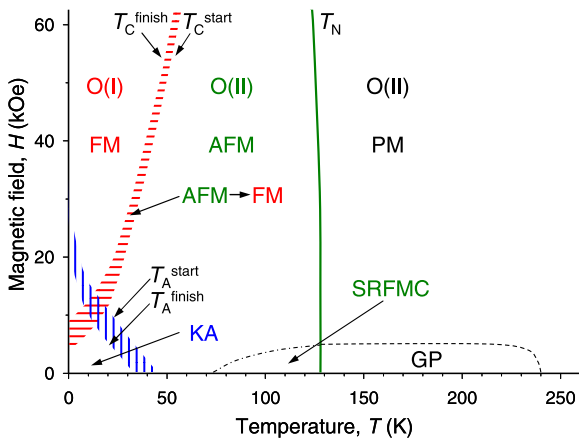
Figure 1. The phase diagram of Gd_5Ge_4 in temperature–magnetic field coordinates [11]. GP refers to the Griffiths phase; SRFMC stands for short range ferromagnetic correlations; PM, AFM, and FM, respectively, are the paramagnetic, antiferromagnetic and ferromagnetic states; O(I) and O(II) indicate crystallography of the relevant phase regions, see figure 2 for details; and KA is the kinetically arrested state. The boundary marked T_N (Néel temperature) delineates the PM ↔ AFM transition; the region over which the magnetostructural transformation between AFM O(II) and FM O(I) states occurs on cooling is hatched horizontally and marked with T_C^{start} and T_C^{finish} (T_C = Curie temperature); and the boundary over which the system freezes and becomes kinetically arrested is hatched vertically and marked with T_A^{start} and T_A^{finish} (T_A = arrest temperature).

magnetic field remains less than ~1 T [12, 13] (see figure 1), or the hydrostatic pressure remains below ~10^2 bar [14]. O(I) and O(II) designate two polymorphic modifications of Gd_5Ge_4, both of which will be briefly described in the next section. The electrical resistivity, heat capacity, magnetization, and linear thermal expansion show that a first order magnetostructural transformation in this compound occurs at atmospheric pressure only when the external magnetic field exceeds ~1 T [6, 12, 15–19]. An x-ray resonant magnetic scattering study [20] confirmed the AFM state as the magnetic ground state of Gd_5Ge_4. Here, the magnetic moments of Gd atoms within each nanolayer (slab) are ferromagnetically aligned parallel to the *c*-axis, while the coupling between neighboring slabs is antiferromagnetic. *In situ* x-ray powder diffraction experiments, carried out isothermally while varying the magnetic field [6, 13], confirmed that a first order phase transition in Gd_5Ge_4 occurs between the Sm_5Ge_4-type [2] AFM state and the Gd_5Si_4-type [21] FM state.

In addition to unusually strong magnetoresponsiveness, the title compound shows quite interesting dynamic behavior. Recent experimental studies [22, 23] indicate that the equilibrium thermodynamic ground state of Gd_5Ge_4 may be FM but this state is avoided due to a kinetic arrest, which occurs over the region delineated by T_A^{start} and T_A^{finish} boundaries in figure 1. Acceptance of this postulate explains why below ~20 K Gd_5Ge_4 shows complex behavior involving irreversible, partially reversible and completely reversible magnetic phase changes [5, 12–18, 24–26] apparently fully coupled to crystallographic phase transitions [6, 13].

When transforming from a true PM state to a long range FM or AFM state, some magnetic materials may adopt an intermediate state where a system exhibits short range FM clustering. The FM correlations are easily observed from the inverse magnetic susceptibility measured in small magnetic fields when the material does not obey the Curie–Weiss law. These properties were predicted by Griffiths, in 1969 [27], to occur in random Ising ferromagnets, when only a fraction of lattice sites are occupied with Ising spins, and hence, the exchange interactions exist only between spins occupying neighboring sites.

Experimentally, short range FM clustering (the Griffiths phase) has been observed in $Tb_2Si_2Ge_2$ [28], Gd_5Ge_4 [29] (see the region marked GP in figure 1), and Dy_5Si_3Ge [30]. Even though none of these compounds resembles a diluted Ising system, the complex and distinctly layered crystallography of R_5T_4 leads to an equally complex anisotropy of the indirect 4f–4f coupling. In other words, interactions within the *ac* planes in the slabs are different from those along the *b* axis between the neighboring slabs. Therefore, when the Gd_5Ge_4 system is in the AFM state, the spins within the same slab align in the same direction (positive intraslab exchange) but they align in the opposite directions between the neighboring slabs indicating that the interslab exchange is negative. As a result of competition between the interslab and intraslab exchange coupling, short range FM clustering (SRFMC region in figure 1) is feasible [28].

In order to better understand the remarkable phenomenology of the $Gd_5Si_xGe_{4-x}$ materials, first principles theories were applied in the recent past, resulting in the calculation of the electronic structure, and the magnetic, magneto-optical, x-ray magnetic circular dichroism, and giant magnetoresistance properties of $Gd_5Si_2Ge_2$ [31–38]. In another recent study [39], electronic structure calculations were coupled to the mean field model in order to analyze finite temperature properties such as magnetization, magnetic free energy and magnetic entropy. This led to a reasonable agreement of the theoretically predicted magnetostructural transition temperature and the magnetocaloric effect in $Gd_5Si_2Ge_2$ with experiment [39]. Also recently, the total energies, exchange splitting, magnetic moments and density of states, DOS, have been calculated in both the O(I) and O(II) structures of Gd_5Ge_4 [40] and $Gd_5Si_{0.5}Ge_{3.5}$ [41]. The total energy analyzed as a function of shear distortion along the *a*-axis indicates a first order transformation in Gd_5Ge_4, supporting the experimental observation. Substantial changes in the exchange splitting, magnetic moments and DOS of 5d electrons of Gd and the 4p electrons of Ge between the two allotropes of Gd_5Ge_4 clearly correlate with the change in the interslab Ge–Ge bonding.

The goal of this work is to understand the origin of ferromagnetism in the O(I) Gd_5Ge_4 and the antiferromagnetism in the O(II) Gd_5Ge_4 through thorough analysis of the electronic structure, band energies, 4f–5d exchange interactions and total energy.

2. Crystallography and theoretical approach

The ground state crystal structure of Gd_5Ge_4 is the orthorhombic (space group symmetry *Pnma*) Sm_5Ge_4-type [2], also known as O(II)-type [21]. Here, the Gd atoms
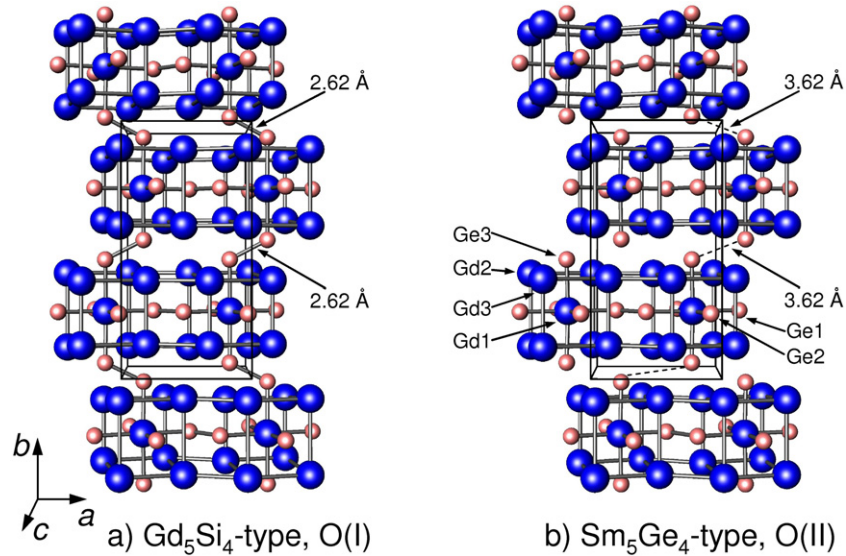
Figure 2. The two polymorphic modifications of Gd$_5$Ge$_4$: (a) the Gd$_5$Si$_4$-type O(I) and (b) the Sm$_5$Ge$_4$-type O(II). Both are layered structures built from nearly identical slabs, and are related to one another by shear displacements of the neighboring slabs. The most drastic change is observed in Ge3–Ge3 interactions between the slabs with the corresponding interatomic distances varying from 2.62 Å in the O(I) to 3.62 Å in the O(II) as indicated in (a) and (b), respectively.

occupy the Sm positions and the Ge atoms occupy the corresponding Ge-sites of the prototype. In this structure, shown in figure 2(b), the Gd atoms occupy three inequivalent sites (Gd1 in 4c, Gd2 and Gd3 in 8d) and Ge atoms also occupy three nonequivalent sites (Ge1 and Ge2 in 4c, and Ge3 in 8d). Altogether, there are 36 atoms (20 Gd and 16 Ge) in the unit cell. In the FM state, the Gd$_5$Ge$_4$ adopts a different orthorhombic structure that belongs to the same space group symmetry, but has the Gd$_5$Si$_4$-type structure, also known as the O(I)-type [21], which is shown in figure 2(a). Both structures are built by stacking pseudo-two-dimensional slabs, each formed by five tightly bound monolayers consisting of Gd, Ge and (Gd + Ge) atoms, along the *b*-axis. Therefore, Gd$_5$Ge$_4$ may exist in a low field AFM O(II) and a high field FM O(I) states. In the FM state, all the slabs are interconnected via short Ge–Ge bonds ($\delta_{Ge-Ge} = 2.62$ Å) but in the AFM state all of these bonds are broken ($\delta_{Ge-Ge} = 3.62$ Å) [6] and replaced by different interslab bonds, e.g. Gd–Gd σ-bonds [12].

During the displacive O(II) $\leftrightarrow$ O(I) transformation, structural changes inside the slabs are negligible [6, 13, 19], but all of the interslab distances, especially the Ge–Ge bonds, are affected to a much greater degree. A 1.2% volume decrease during the AFM O(II) $\rightarrow$ FM O(I) transformation is unusual because, typically, the phase volume increases upon ferromagnetic ordering [42], but this relationship between the phase volumes is similar to other R$_5$Si$_x$Ge$_{4-x}$ compounds [5, 43–45]. The change in the magnetism from the AFM state in the O(II) allotrope to the FM state in the O(I) polymorph is related to the changes in the local exchange splitting, local magnetic moments of 5d states, and indirect 4f–4f magnetic exchange coupling, all of which are due to the phase volume change and the dramatic change in the interslab Ge–Ge bond lengths [40].

The local spin density approximation with the on-site Coulomb parameter (LSDA + *U*) correlated band approach [46, 47] has been employed to investigate the electronic and magnetic properties of the Gd$_5$Ge$_4$ system as a function of crystallography. The advantage of this approach over LSDA and details of its implementation have been discussed in our recent publication [39], see also references therein. The calculations have been performed using the scalar relativistic version (which includes the mass velocity and Darwin correction terms) of the LSDA + *U* method implemented in the tight binding linear muffin-tin orbital (TB-LMTO) schemes [48]. We employed *U* = 6.7 eV and *J* = 0.7 eV for the proper positioning of the occupied and unoccupied 4f bands of Gd atoms in Gd$_5$Ge$_4$ [46]. The Langreth, Mehl and Hu [49–51] parameterization for the exchange correlation functional has been employed because it resulted in estimates that were closer to experimental values for the transition temperatures in the related Gd$_5$Si$_2$Ge$_2$ system [39] as compared to the von Barth and Hedin [52] local exchange correlation, or the Perdew and Wang [53, 54] nonlocal exchange correlation, which respectively, underestimate and overestimate the transition temperature. A total of 125 special *k* points in the irreducible part of the Brillouin zone were used for *k* space integrations.

The magnetic interactions in rare earth based systems are indirect, i.e. Ruderman–Kittel–Kasuya–Yosida (RKKY) Gd 4f–Gd 4f exchange mediated by spin polarized conduction electrons. The mathematical details of computing RKKY interactions can be found in standard text books (e.g. see [55]). In this paper we estimate the Gd 4f–Gd 4f indirect exchange by calculating the 4f–5d exchange interactions of different Gd atoms in the O(I) and O(II) structures of Gd$_5$Ge$_4$. For theoretical details and examples of application to some rare earth based materials we refer interested readers to [56–59].
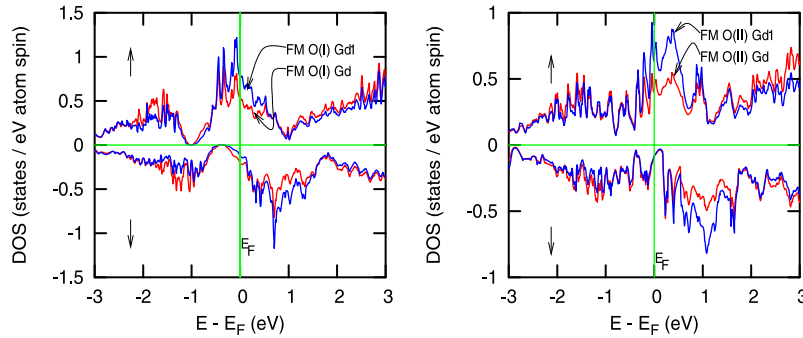
Figure 3. Comparison of the average 5d DOS of all Gd atoms with the 5d DOS of the Gd1 atom in the FM O(I) (left) and FM O(II) (right) structures. See [40] for the location of Gd1-3 and Ge1-3 atoms in each of the two polymorphs of Gd_5Ge_4. The up- and down-arrow represent the majority (spin up) and minority (spin down) DOS respectively.

3. Results and discussion

In a recent work [40] the role of shear distortions in the stability of the two polymorphic modifications of Gd_5Ge_4 has been studied by analyzing the total energy. The total energy as a function of shear distortion of the slabs indicates a first order transformation from the AFM O(II) Gd_5Ge_4 to FM O(I) Gd_5Ge_4 supporting experimental observations. As reported in [40], the total energy for the AFM O(II) Gd_5Ge_4 is lower by 0.020 eV/Gd compared to that of the FM O(I) Gd_5Ge_4 indicating that the AFM O(II) Gd_5Ge_4 is the ground state structure of Gd_5Ge_4. The AFM structure was constructed by doubling the unit cell along the *b*-direction and assigning ↑↑ (spin up) configurations to the Gd atoms in one slab and ↓↓ (spin down) configurations in the neighboring slab.

Because of the asymmetry in the Gd–Ge–Ge–Gd bonding within and between the slabs in the O(II) structure, these interactions should differ from the O(I) structure, whereas the Gd–Ge–Ge–Gd bonding inside and between the slabs is the same. The role of the Ge 4p states in RKKY exchange arises from their hybridization with the 5d states of the Gd atoms. The occupied 4f states in Gd_5Ge_4, which are far below the Fermi level, are localized and carry a magnetic moment of 7 μ_B/Gd thus acting as an effective field to spin polarize 5d electrons. The energy difference between the band centers of the atom projected 5d states of the Gd atoms and 4p states of the Ge atoms shows that hybridization between spin up 5d states and spin up 4p states is the same in both the FM O(I) and FM O(II) structures. But there is a stronger hybridization between spin down 5d states and spin down 4p states in the O(II) structure than in the O(I) structure [40].

In order to examine the difference in the spin polarization of 5d electrons in the O(I) and O(II) structures of Gd_5Ge_4, one needs to consider the density of states. The occupied and unoccupied 4f bands are, respectively, far below and above the Fermi level in both structures. Yet, the occupied 4f band centers in the O(I) structure are higher in energy by 3.8% (Gd1), 0.9% (Gd2) and 0.6% (Gd3) compared to the corresponding Gd atoms in the O(II) structure. Because of this, the spin polarization of corresponding 5d electrons in the two structures is different. As reflected in 5d–4p hybridization, this is primarily caused by the variability in Gd–Ge–Ge–Gd

bonding. Figure 3 compares the average DOS of all Gd atoms and DOS for the Gd1 atom (the latter plays a critical role in forming –Gd–Ge–Ge–Gd– networks that are continuous in the O(I) Gd_5Ge_4 but are limited to individual slabs in the O(II) Gd_5Ge_4). The DOS behave similarly but the average DOS of all Gd atoms is lower than that of the Gd1 atom at the Fermi level in both allotropes. Similarity of the average DOS of all Ge atoms and that of the Ge3 atom (the changes in bonding between the Ge3 atoms either destroy or reform the continuity of the –Gd–Ge–Ge–Gd– networks) has also been observed (not shown). These observations indicate that the Gd1 and Ge3 play dominant roles in the magnetism of Gd_5Ge_4. It should be noted that the spin down 5d DOS of Gd in the FM O(I) just below the Fermi level is zero in the energy range −0.3 to −0.5 eV showing that all the electrons in this energy range are confined in the spin up band (figure 3, left panel). But the spin down 5d DOS of Gd in the FM O(II) has a nonzero peak in the energy range −0.1 to −0.2 eV, where some electrons occupy the spin down band (figure 3, right panel). As a result, the 5d-Gd magnetic moment is much lower in the FM O(II) than in the FM O(I).

Figure 4 compares the average 5d DOS of all Gd atoms and average 4p DOS of all Ge atoms in the FM O(I) and FM O(II) structures. Both are completely rearranged when the structure changes from the O(I) to the O(II). During this transformation there is a 24% decrease in the DOS (E_F) and also a 16% decrease in the band splitting of Gd atoms. Due to these two factors there is an average 50% decrease of the 5d magnetic moments of Gd atoms in the FM O(II) Gd_5Ge_4 compared to the FM O(I) Gd_5Ge_4, as indicated above.

The integrated number of electrons (including s, p, d and f electrons) up to the Fermi level within the atomic spheres of all atoms in both the O(II) and O(I) Gd_5Ge_4 is important in order to understand how the occupied majority (spin up) and minority (spin down) bands affect the magnetism of Gd_5Ge_4. Figure 5 shows the difference of the total integrated number of electrons between the O(I) and O(II) Gd_5Ge_4 imposing FM order in both structures. In the O(I) structure, the total number of spin up electrons of Gd2 and Gd3 is larger than the number of corresponding electrons in the O(II) structure, whereas the total number of spin down electrons of Gd1 of the O(II) structure is larger than the same in the O(I) structure. The total
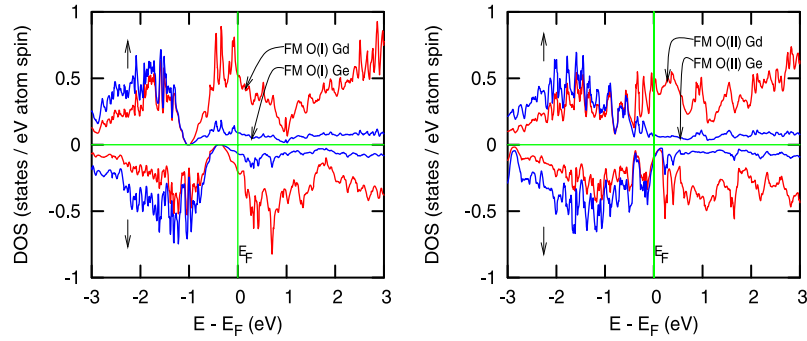
Figure 4. Comparison of the average 5d DOS of all Gd atoms and average 4p DOS of all Ge atoms in the FM O(I) and FM O(II) structures of Gd_5Ge_4.
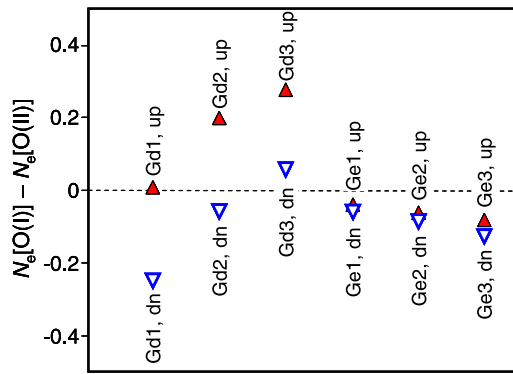

Figure 5. Differences of the integrated number of electrons within the atomic spheres of each atom between the O(I) and the O(II) Gd_5Ge_4. The upward pointing (filled) triangles correspond to the spin up electrons, while the downward pointing triangles correspond to the spin down electrons.
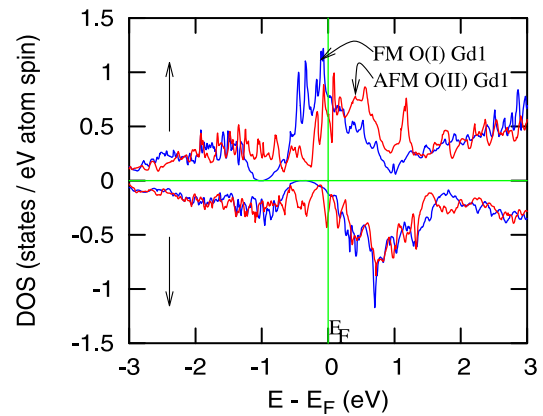

Figure 6. Comparison of the 5d DOS of Gd1 in the FM O(I) Gd_5Ge_4 and AFM O(II) Gd_5Ge_4.

number of spin down electrons of the Ge3 atom in the O(II) phase is the greatest among all Ge atoms in both the O(I) and O(II) Gd_5Ge_4. Most of the contributions in the spin down electrons of Gd1 and Ge3 in the O(II) structure come from 5d and 4p states, respectively. Therefore, a large number of spin down electrons of Gd1 and Ge3 in a structure with long, nonbonded Ge3–Ge3 pairs indicates a reduction of the occupied states in the spin up bands, thus resulting in the destruction of the FM order between the slabs in the O(II) structure. On the other hand, the large number of electrons in the spin up bands of the Gd atoms in a structure with short Ge3–Ge3 pairs is consistent with the FM coupling between the slabs.

The reduction of moment is linked with the role of the Ge atoms in the FM O(II) structure. When the interslab Ge–Ge bonding is weak, the 5d bands of Gd atom linking neighboring slabs reshuffle and interslab Ge 4p bands are pushed towards the higher energy. It is evident from figure 4 that the Ge 4p bands are similar in shape to the Gd 5d bands at and just below the Fermi level. The spin up electrons from 5d bands of Gd are then transferred to these hybridized spin down 5d Gd and Ge 4p bands, and therefore, the magnetic moment of 5d Gd decreases in the FM O(II) structure.

Figure 6 shows the 5d DOS of Gd1 atoms in the FM O(I) and AFM O(II) structures. The spin up 5d DOS of Gd1 at the

Fermi level is lower by 31% in the AFM O(II) than in the FM O(I). The band splitting of 5d Gd1 is also lower by 23% in the AFM O(II) compared to the FM O(I). These factors explain the origin of the 67% decrease of the indirect 4f–4f exchange coupling energy in the Gd atoms of the AFM O(II) compared to the FM O(I) Gd_5Ge_4 noted in [40].

Recent experiments [29] indicate that short range FM clustering occurs in both the AFM and PM phases of the O(II) Gd_5Ge_4. Short range magnetic ordering or clustering has been treated only in simple body centered and face centered cubic structures using first principles configurational averaging methods, e.g. Korringa–Kohn–Rostoker coherent potential approximation (KKR–CPA) [60] and augmented space recursion (ASR) [61, 62]. To date, there have been no theoretical efforts aimed at explaining FM clustering in materials of this complexity.

However, qualitative analysis of short range FM clustering in the O(II) Gd_5Ge_4 may be achieved by analyzing band energies and exchange interactions between Gd atoms within and between the slabs. Here, the positive (ferromagnetic) indirect 4f–4f exchange between the nearest neighbor Gd atoms surrounding Gd1, i.e. those Gd atoms that belong to the same slab, is taken as a signature of short range FM clustering. Before this analysis, we examine how the total energy varies as a function of distance between the neighboring slabs. The
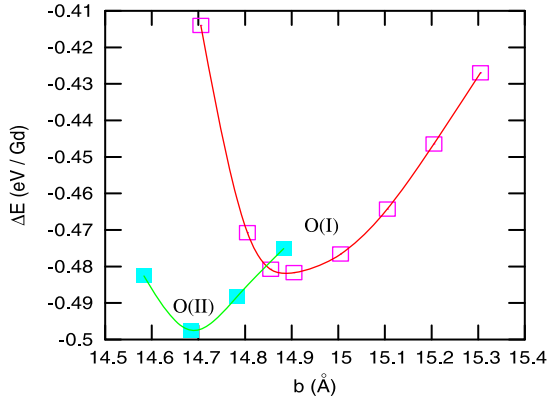
Figure 7. Total energy variation in FM Gd_5Ge_4 as a function of lattice constant b.

orthorhombic ($Pnma$) structure has been converted into the equivalent triclinic (P1) structure so that each of the 36 atoms in the unit cell of Gd_5Ge_4 is formally no longer equivalent to any other atom in the same unit cell. This makes all of the atoms distinguishable. Furthermore, the separation between the neighboring slabs, without affecting the structure of each slab, can be changed by changing the lattice constant b. While changing b, the relative y-coordinates of the Ge and Gd atoms located in the neighboring slabs (slabs I and II) have been modified as follows to maintain the integrity of each slab.

For the atoms in slab I,

$$ y_2 = \frac{\frac{1}{4}b_2 - \delta}{b_2} \qquad \text{with } \delta = \tfrac{1}{4}b_1 - B. $$

For the atoms in slab II,

$$ y_2 = \frac{\frac{3}{4}b_2 - \delta}{b_2} \qquad \text{with } \delta = \tfrac{3}{4}b_1 - B $$

where b_1 (b_2) and y_1 (y_2) are the old (new) lattice constant and relative coordinate, respectively, and $B = b_1 y_1$.

The total energy variation as a function of lattice constant b (figure 7) indicates two minima at $b = 14.905$ Å and $b = 14.683$ Å corresponding to the FM O(I) Gd_5Ge_4 and FM O(II) Gd_5Ge_4 respectively. For these calculations, other lattice constants a and c and atomic coordinates x and z were kept equal to the experimental values of the O(I) Gd_5Ge_4 and O(II) Gd_5Ge_4 structures, respectively [6, 13]. The calculated values of lattice constants b are in qualitative agreement with the experimental values of 14.805 Å and 14.783 Å for the O(I) and O(II), respectively. The total energy minimum for the O(II) is lower by 0.013 eV/Gd than the O(I) structure once again indicating that O(II) is the ground state structure. Even though, the two polymorphs in [40] were modeled by shearing the slabs while keeping the phase volumes constant, the result obtained here is in agreement with [40] despite the fact that now the phase volume of each phase has been varied.

The individual slabs contain two-dimensional networks –Gd1–Ge2–Ge1–Gd1– that have short, strongly bonded Ge1–Ge2 pairs in both the O(I) and O(II) structures; but the neighboring slabs are connected by either the short, strongly

bonded Ge3–Ge3 pairs in the O(I), or the long, nonbonded Ge3–Ge3 pairs in the O(II) structures. The Gd1 atoms are in the middle of each slab, and therefore, the nearest neighbor sphere of the Gd1 atoms falls within the same slab in both structures. The next nearest neighbor sphere of the Gd1 atoms includes atoms from the neighboring slabs on each side, and the spheres are asymmetrical in the O(II) structure but symmetrical in the O(I) structure with respect to the –Gd–Ge–Ge–Gd– linkage. The differences in band energies between Gd1 and its nearest and next nearest neighbor Gd atoms show how they interact with one another when neighboring slabs interact via either the short or the long Ge3–Ge3 bonds. The atom projected band energy can be defined in terms of the atom projected density of states ($D^i(E)$) and is given as

$$ E_b^i = \int_{-\infty}^{E_F} E D^i(E) \, dE. $$

In the O(I) Gd_5Ge_4, the difference in band energy between the central Gd1 atom and the nearest neighbor Gd atoms is 0.698 eV and between Gd1 and the next nearest neighbor Gd atoms it is 0.366 eV. They are 0.202 eV and -0.944 eV, respectively, in the O(II) Gd_5Ge_4. This variation of band energies indicates that the change in the Ge3–Ge3 bonding together with the phase volume change greatly affects the relative band energies of the next nearest neighbor Gd atoms in both allotropes of Gd_5Ge_4. The signs of the band energy differences point to the long range FM order in the O(I) Gd_5Ge_4, while only a short range FM order is supported in the O(II) Gd_5Ge_4. With this, one may argue that, because of the asymmetry in bonding of Ge–Ge pairs, the interslab interactions and therefore magnetic structures of the O(I) and O(II) polymorphs of Gd_5Ge_4 are different, as is indeed observed experimentally [20].

We now analyze the indirect 4f–4f exchange interactions in both structures of Gd_5Ge_4. As stated above, the nearest neighbor atoms of Gd1 always belong to the same slab and the next nearest neighbor atoms are from neighboring slabs. Assuming that the differences in 4f–5d exchange energies between Gd1 and its nearest neighbor Gd atoms (δ_{4f-5d}^{NN}) reflects the intraslab 4f–4f exchange, then the same differences between Gd1 and its next nearest neighbor Gd atoms (δ_{4f-5d}^{NNN}) reflects the interslab 4f–4f exchange. In the O(I) Gd_5Ge_4, $\delta_{4f-5d}^{NN} = 0.070$ eV and $\delta_{4f-5d}^{NNN} = 0.069$ eV. They change to 0.042 eV and -0.013 eV, respectively, in the O(II) Gd_5Ge_4. The positive nearest and next nearest neighbor 4f–4f exchange interactions are consistent with the long range FM order in the O(I) Gd_5Ge_4, while only a positive nearest neighbor 4f–4f exchange interaction supports a short range FM order within the slabs of the O(II) Gd_5Ge_4, which is exactly what is observed experimentally [12, 20, 29]. The negative value of δ_{4f-5d}^{NNN} in the O(II) Gd_5Ge_4, which includes the interslab Gd atoms explains the origin of the antiferromagnetic ground state.

In order to validate these conclusions, the total energies were calculated for different spin structures using the low symmetry ($P1$) model structurally equivalent to the real $Pnma$ space group as explained above. In the O(I) Gd_5Ge_4, the total energy of the FM structure is lower than the total energy of the AFM structure constructed so that 10 Gd atoms/cell that

belong to the same slab are aligned ferromagnetically but the remaining 10 Gd atoms that belong to the neighboring slab are aligned ferromagnetically in the opposite direction. For the O(II) Gd_5Ge_4, the result is opposite, i.e. AFM arrangement of the ferromagnetically ordered slabs results in lower total energy. Furthermore, if the AFM structure is modeled by individual slabs being AFM (i.e. 5 Gd spins in each slab are up and 5 are down), then the total energy is higher than the corresponding FM structures regardless of crystallography. These results, therefore, confirm both inter and intraslab FM order in the O(I) Gd_5Ge_4 and intraslab FM order but interslab AFM order in the O(II) Gd_5Ge_4.

4. Conclusions

The location of the band centers of 5d Gd and 4p Ge and the energy difference between them indicate that spin down 5d states of Gd1 and spin down 4p states of Ge3 in the O(II) Gd_5Ge_4 are strongly hybridized. When the O(I) Gd_5Ge_4 transforms into the O(II) Gd_5Ge_4, the indirect exchange interaction between 4f spins of Gd atoms substantially decreases, resulting in the rearrangement of the 5d Gd and 4p Ge bands with a considerable decrease in the 5d DOS of Gd atoms and reduced band splitting at the Fermi level. The integrated numbers of electrons in the minority and majority bands differ substantially from one allotrope to another, showing different magnetic moments. The indirect 4f–4f exchange interaction analysis from the calculations of 4f–5d exchange energies and the total energy of different spin configurations followed by band energy analysis indicates short range ferromagnetic but long range antiferromagnetic coupling between Gd atoms in the O(II) Gd_5Ge_4. Only ferromagnetic coupling is found in the O(I) structure of Gd_5Ge_4.

Acknowledgments

References

[1] Bader S D 2006 *Rev. Mod. Phys.* **78** 1
[2] Smith G S, Tharp A G and Johnson Q 1967 *Acta Crystallogr.* **22** 940
[3] Holtzberg F, Gambino R J and McGuire T R 1967 *J. Phys. Chem. Solids* **28** 2283
[4] Pecharsky V K and Gschneidner K A Jr 1997 *Phys. Rev. Lett.* **78** 4494
[5] Morellón L, Algarabel P A, Ibarra M R, Blasco J, García-Landa B, Arnold Z and Albertini F 1998 *Phys. Rev. B* **58** R14721
[6] Pecharsky V K, Holm A P, Gschneidner K A Jr and Rink R 2003 *Phys. Rev. Lett.* **91** 197204
[7] Gschneidner K A Jr, Pecharsky V K and Tsokol A O 2005 *Rep. Prog. Phys.* **68** 1479
[8] Fujita A, Fujieda S, Hasegawa Y and Fukamichi K 2003 *Phys. Rev. B* **67** 104416
[9] Tegus O, Brück E, Buschow K H J and de Boer F R 2002 *Nature* **415** 150
[10] de Campos A *et al* 2006 *Nat. Mater.* **5** 802
[11] Pecharsky V K and Gschneidner K A Jr 2007 *Pure Appl. Chem.* **79** 1383
[12] Levin E M, Pecharsky V K, Gschneidner K A Jr and Miller G J 2001 *Phys. Rev. B* **64** 235103
[13] Mudryk Ya, Holm A P, Gschneidner K A Jr and Pecharsky V K 2005 *Phys. Rev. B* **72** 064442
[14] Magen C, Arnold Z, Morellon L, Skorokhod Y, Algarabel P A, Ibarra M R and Kamarad J 2003 *Phys. Rev. Lett.* **91** 207202
[15] Levin E M, Gschneidner K A Jr and Pecharsky V K 2002 *Phys. Rev. B* **65** 214427
[16] Magen C, Morellon L, Algarabel P A, Marquina C and Ibarra M R 2003 *J. Phys.: Condens. Matter* **15** 2389
[17] Chattopadhyay M K *et al* 2004 *Phys. Rev. B* **70** 214421
[18] Hardy V *et al* 2004 *Phys. Rev. B* **69** 020407(R)
[19] Holm A P, Pecharsky V K, Gschneidner K A Jr, Rink R and Jirmanus M N 2004 *Rev. Sci. Instrum.* **75** 1081
[20] Tan L *et al* 2005 *Phys. Rev. B* **71** 214408
[21] Pecharsky V K and Gschneidner K A Jr 1997 *J. Alloys Compounds* **260** 98
[22] Roy S B, Chattopadhyay M K, Chaddah P, Moore J D, Perkins G K, Cohen L F, Gschneidner K A Jr and Pecharsky V K 2006 *Phys. Rev. B* **74** 012403
[23] Roy S B, Chattopadhyay M K, Banerjee A, Chaddah P, Moore J D, Perkins G K, Cohen L F, Gschneidner K A Jr and Pecharsky V K 2007 *Phys. Rev. B* **75** 184410
[24] Tang H, Pecharsky V K, Gschneidner K A Jr and Pecharsky A O 2004 *Phys. Rev. B* **69** 064410
[25] Levin E M, Gschneidner K A Jr, Lograsso T A, Schlagel D L and Pecharsky V K 2004 *Phys. Rev. B* **69** 144428
[26] Casanova F, Labarta A and Batlle X 2005 *Phys. Rev. B* **72** 172402
[27] Griffiths R B 1969 *Phys. Rev. Lett.* **23** 17
[28] Magen C, Algarabel P A, Morellon L, Araújo J P, Ritter C, Ibarra M R, Pereira A M and Sousa J B 2006 *Phys. Rev. Lett.* **96** 167201
[29] Ouyang Z W, Pecharsky V K, Gschneidner K A Jr, Schlagel D L and Lograsso T A 2006 *Phys. Rev. B* **74** 094404
[30] Nirmala R, Mudryk Ya, Pecharsky V K and Gschneidner K A Jr 2007 *Phys. Rev. B* **76** 104417
[31] Pecharsky V K, Samolyuk G D, Antropov V P, Pecharsky A O and Gschneidner K A Jr 2003 *J. Solid State Chem.* **171** 57
[32] Samolyuk G D and Antropov V P 2002 *J. Appl. Phys.* **91** 8540
[33] Samolyuk G D and Antropov V P 2005 *J. Appl. Phys.* **97** 10A310
[34] Harmon B N and Antonov V N 2002 *J. Appl. Phys.* **91** 9815
[35] Harmon B N and Antonov V N 2003 *J. Appl. Phys.* **93** 4678
[36] Tang H, Pecharsky V K, Samolyuk G D, Zou M, Gschneidner K A Jr, Antropov V P, Schlagel D L and Lograsso T A 2004 *Phys. Rev. Lett.* **93** 237203
[37] Skorek G, Deniszczyk J and Szade J 2002 *J. Phys.: Condens. Matter* **14** 7273
[38] Haskel D, Lee Y B, Harmon B N, Islam Z, Lang J C, Srajer G, Mudryk Ya, Gschneidner K A Jr and Pecharsky V K 2007 *Phys. Rev. Lett.* **98** 247205
[39] Paudyal D, Pecharsky V K, Gschneidner K A Jr and Harmon B N 2006 *Phys. Rev. B* **73** 144406
[40] Paudyal D, Pecharsky V K, Gschneidner K A Jr and Harmon B N 2007 *Phys. Rev. B* **75** 094427
[41] Mudryk Ya, Paudyal D, Pecharsky V K and Gschneidner K A Jr 2008 *Phys. Rev. B* **77** 024408
[42] Lindbaum A and Rotter M 2002 *Hand Book of Magnetic Materials* vol 14, ed K H J Buschow (Amsterdam: Elsevier) chapter 4, p 307

[43] Choe W, Pecharsky V K, Pecharsky A O, Gschneidner K A Jr, Young V G Jr and Miler G J 2000 *Phys. Rev. Lett.* **84** 4617
[44] Ritter C, Morellon L, Algarabel P A, Magen C and Ibarra M R 2002 *Phys. Rev.* B **65** 094405
[45] Garlea V O, Zarestky J L, Zones C Y, Lin L-L, Schlagel D L, Lograsso T A, Tsokol A O, Pecharsky V K, Gschneidner K A Jr and Stassis C 2005 *Phys. Rev.* B **72** 104431
[46] Anisimov V I, Aryasetiawan F and Lichtenstein A I 1997 *J. Phys.: Condens. Matter.* **9** 767
[47] Harmon B N, Antropov V P, Lichtenstein A I, Solovyeb I V and Anisimov V I 1995 *J. Phys. Chem. Solids* **56** 1521
[48] Andersen O K and Jepsen O 1984 *Phys. Rev. Lett.* **53** 2571
[49] Langreth D C and Mehl M J 1981 *Phys. Rev. Lett.* **47** 446
[50] Langreth D C and Mehl M J 1983 *Phys. Rev.* B **28** 1809
[51] Hu C D and Langreth D C 1985 *Phys. Scr.* **32** 391
[52] von Barth U and Hedin L 1972 *J. Phys. C: Solid State Phys.* **5** 1629
[53] Perdew J P 1986 *Phys. Rev.* B **33** 8822
[54] Perdew J P and Wang Y 1986 *Phys. Rev.* B **33** 8800
[55] White R M 2007 *Quantum Theory of Magnetism* 3rd edn (Berlin: Springer) chapter 9, p 286
[56] Brooks M S S and Johansson B 1993 *Hand Book of Magnetic Materials* vol 7, ed K H J Buschow (North-Holland: Elsevier) chapter 3, p 139
[57] Jensen J and Mackintosh A R 1994 *Rare Earth Magnetism Structures and Excitations* (Oxford: Clarendon) chapter 1, p 45
[58] Richter M 1998 *J. Phys. D: Appl. Phys.* **31** 1017
[59] Ahuja R, Auluck S, Johansson B and Brooks M S S 1994 *Phys. Rev.* B **50** 5147
[60] Staunton J B, Ling M F and Johnson D D 1997 *J. Phys.: Condens. Matter* **9** 1281
[61] Paudyal D, Saha-Dasgupta T and Mookerjee A 2004 *J. Phys.: Condens. Matter* **16** 2317
[62] Paudyal D, Saha-Dasgupta T and Mookerjee A 2004 *J. Phys.: Condens. Matter* **16** 7247